The ISME Journal (2007) 1, 551–565

www.nature.com/ismej

ORIGINAL ARTICLE

Hydrogen is the central free intermediate during lignocellulose degradation by termite gut symbionts

Michael Pester and Andreas Brune
Department of Biogeochemistry, Max Planck Institute for Terrestrial Microbiology, Karl-von-Frisch-Strasse, Marburg, Germany

The key role of free hydrogen in the digestion of lignocellulose by wood-feeding lower termites and their symbiotic gut microbiota has been conceptually outlined in the past decades but remains to be quantitatively analyzed *in situ*. Using *Reticulitermes santonensis*, *Zootermopsis nevadensis* and *Cryptotermes secundus*, we determined metabolite fluxes involved in hydrogen turnover and the resulting distribution of H_2 in the microliter-sized gut. High-resolution hydrogen microsensor profiles revealed pronounced differences in hydrogen accumulation among the species (from $<$1 kPa to the saturation level). However, flux measurements indicated that the hydrogen pool was rapidly turned over in all termites, irrespective of the degree of accumulation. Microinjection of radiotracers into intact guts confirmed that reductive acetogenesis from CO_2 dominated hydrogen consumption, whereas methanogenesis played only a minor role. Only negligible amounts of H_2 were lost by emission, documenting an overall equilibrium between hydrogen production and consumption within the gut. Mathematical modeling revealed that production dominates in the gut lumen and consumption in the gut periphery for *R. santonensis* and *Z. nevadensis*, explaining the large accumulation of H_2 in these termites, whereas the moderate hydrogen accumulation in *C. secundus* indicated a more balanced radial distribution of the two processes. Daily hydrogen turnover rates were 9–33 m^3 H_2 per m^3 hindgut volume, corresponding to 22–26% of the respiratory activity of the termites. This makes H_2 the central free intermediate during lignocellulose degradation and the termite gut—with its high rates of reductive acetogenesis—the smallest and most efficient natural bioreactor currently known.
The ISME Journal (2007) **1,** 551–565; doi:10.1038/ismej.2007.62; published online 2 August 2007
Subject Category: microbial ecosystem impacts
Keywords: hydrogen turnover; metabolite fluxes; methanogenesis; quantitative degradation model; reductive acetogenesis; symbiosis

Introduction

Termites inhabit about two-thirds of Earth's terrestrial surface and play important roles in the global carbon cycle (Lee and Wood, 1971; Wood and Sands, 1978; Collins and Wood, 1984; Sanderson, 1996; Bignell and Eggleton, 2000). Recently, wood-feeding termites received additional attention because lignocellulose degradation by their symbiotic gut microbiota presumably produces large amounts of hydrogen, an emerging 'clean' energy carrier (Dunn, 2002).

Lignocellulose is the most abundant renewable resource of the biosphere. It consists mainly of cellulose and hemicelluloses, both of which are degraded with high efficiency during gut passage by the termite (65–99%, reviewed in Breznak and Brune, 1994). Although termites secrete their own cellulases and hemicellulases into foregut and midgut (Inoue *et al.*, 1997; Watanabe and Tokuda, 2001; Tokuda *et al.*, 2004, 2005), it is generally accepted that most of the polysaccharide degradation in lower termites occurs in the enlarged hindgut (Inoue *et al.*, 1997; Tokuda *et al.*, 2005), a bioreactor-like compartment with increased retention time and tightly packed with microorganisms (Breznak and Brune, 1994; Brune, 1998).

In lower termites, the hindgut microbiota comprises flagellate protozoa, which are considered the primary agents of lignocellulose degradation, and a great variety of prokaryotes, whose particular function is often unknown (Breznak, 2000; Brune and Stingl, 2005; Brugerolle and Radek, 2006; Brune, 2006). About 70 years ago, Robert E Hungate was the first to realize that H_2, CO_2, and acetate are the main degradation products formed by the large cellulolytic protozoa (Hungate, 1939, 1943) that occupy the

Correspondence: A Brune, Department of Biogeochemistry, Max Planck Institute for Terrestrial Microbiology, Karl-von-Frisch-Strasse, 35043 Marburg, Germany.
E-mail: brune@mpi-marburg.mpg.de
Received 10 April 2007; revised 13 June 2007; accepted 25 June 2007; published online 2 August 2007

bulk of the hindgut volume of all lower termites (reviewed by Brune and Stingl, 2005). *In vitro* studies on *Trichomitopsis termopsidis* and *Trichonympha sphaerica* added support for Hungate's observations (Yamin, 1980, 1981; Odelson and Breznak, 1985), but owing to the difficulties in cultivating termite gut protozoa, there are no metabolic studies on any other flagellate species. Hydrogen production from maltose has been shown also for the termite gut spirochete *Treponema azotonutricium* (Graber *et al.*, 2004), but the significance of prokaryotes as hydrogen source is not clear.

In contrast, the role of prokaryotes as a hydrogen sink is well established. Diluted gut homogenates of various lower termites showed high potential rates of reductive acetogenesis from H_2 and CO_2, whereas hydrogenotrophic methanogenesis was less pronounced (Breznak and Switzer, 1986; Brauman *et al.*, 1992). This was consistent with the hypothesis that the termite hindgut functions as a homoacetogenic fermentor, with acetate being the major energy source of the termite (Odelson and Breznak, 1983). In this context, it was assumed that the fermentation is a syntrophic process, where the H_2 produced by the protozoa is subsequently consumed by homoacetogens (Breznak, 1994).

With the introduction of *in situ* methods to termite gut research, which allowed determination of substrate gradients and metabolite fluxes while maintaining the integrity of the microliter-sized gut environment, a more detailed picture of the degradation process in the hindgut became apparent. Oxygen microsensor measurements revealed that the hindgut is a gradient system composed of an anoxic gut center and a microoxic periphery (Brune *et al.*, 1995; Brune, 1998). This has implications on the metabolism occurring in these different regions, as shown by microinjection of radiolabeled metabolites into the hindgut of *Reticulitermes flavipes* (Tholen and Brune, 2000). In particular, lactate was identified as a relevant intermediate that is apparently degraded by propionigenic bacteria located in the microoxic periphery—a finding that demonstrates that the gut metabolism is more complex than merely catalyzing a strictly homoacetogenic fermentation. In addition, the first hydrogen microsensor measurements with *R. flavipes* (Ebert and Brune, 1997) revealed that the hydrogen partial pressure is not in a range where it would allow syntrophic interactions (<0.1 kPa; Schink, 1997), but accumulates to high concentrations in the gut center.

Thus, the gut metabolism continues to require examination—our concept of it, further development to a robust quantitative model. In this study, we analyzed hydrogen turnover and the resulting intestinal distribution of H_2 using an *in situ* approach. Since it was not possible to label the hydrogen pool directly, we determined the rates of hydrogen-consuming processes by microinjection of ^{14}C-labeled substrates. Subsequently, the spatial distribution of net hydrogen production within the hindgut was analyzed by mathematical modeling. To cover a broad taxonomic range of lower termites, we studied *Reticulitermes santonensis*, *Zootermopsis nevadensis* and *Cryptotermes secundus*, representatives of the three families (Rhinotermitidae, Termopsidae and Kalotermitidae) with the highest number of species (Kambhampati and Eggleton, 2000).

Materials and methods

Termites

R. santonensis was collected in the Forêt de la Coubre, near Royan, France. *Z. nevadensis* stemmed from the Los Padres National Forest in California, USA. *C. secundus* stemmed from a mangrove forest near Darwin, Australia. All termites were maintained on a diet of pine wood (*Pinus silvestris* for *R. santonensis* and *Z. nevadensis*, *Pinus radiata* for *C. secundus*). The species identity of the termites was confirmed by partial sequencing of their *cox2* gene (Pester and Brune, 2006).

Hindgut dimensions were determined with freshly dissected guts immersed in a drop of insect Ringer's solution (Brune *et al.*, 1995), using a dissecting microscope equipped with a calibrated eyepiece reticle. Gut volumes were estimated by approximation to simple geometrical shapes.

Microelectrode measurements

Design and characteristics of polarographic H_2 microelectrodes and redox microelectrodes used in this study were as described by Ebert and Brune (1997). H_2 microelectrodes were calibrated using deionized water continuously flushed with air–hydrogen mixtures of different hydrogen partial pressures (P_{H2} in kPa: 0.0; 4.9; 9.4; 13.5; 100.0) and gave a linear response from 0 to 100 kPa H_2. The lower detection limit is 0.1 kPa H_2. Air–hydrogen mixtures were produced from synthetic air (purity $\geqslant$99.999 vol%) and H_2 (purity $\geqslant$99.999 vol%) using digital mass flow controllers (Bronkhorst, Reinach, Switzerland) and were subsequently introduced directly into the calibration chamber (Ebert and Brune, 1997). Redox microelectrodes were calibrated using quinhydrone dissolved to saturation in commercial pH calibration solutions (pH 4.0–7.0). For the measurements, termite guts were dissected and embedded fully extended in agarose-solidified insect Ringer's solution (Brune *et al.*, 1995).

Gas emission from termites

Gas emission from living termites was analyzed using an experimental setup as described previously (Schmitt-Wagner and Brune, 1999), except that sample volumes were 200 μl. Emission rates were corrected for the dilution effects caused by the sampling procedure and for the basal concentration of the respective gas in the headspace of the incubation vial at the onset of the experiment.

H_2 was measured by gas chromatography using a packed column (Mol Sieve 5A, 80/100 mesh; 70 cm × 6.35 mm) and a reduction gas detector (RGD2, Trace Analytical, CA, USA). The injector temperature was room temperature, the column temperature was 90°C and the temperature of the HgO bed was 280°C. The carrier gas was synthetic air with a flow rate of 20 ml min^{-1}. The lower detection limit was 0.04 ppmv H_2.

CH_4 was measured by gas chromatography using a packed column (Mol Sieve 5A, 80/100 mesh; 30 m × 0.32 mm) and a flame ionization detector. The injector and column temperatures were 100°C, and the detector temperature was 140°C. The carrier gas was helium with a flow rate of 20 ml min^{-1}.

CO_2 was measured by gas chromatography using a packed column (Porapack Q column, 80/100 mesh; 274 cm × 3.18 mm) and a methanizer coupled to a flame ionization detector. The column temperature was 80°C; the carrier gas was 100% hydrogen with a flow rate of 21.5 ml min^{-1}. Samples were directly injected onto the column.

For all gas measurements, the system was routinely calibrated with certified standards (H_2 and CH_4: 2, 50, 1000 ppmv; CO_2: 500, 1000, 2000 ppmv), always resulting in a linear response. All calibration gases were from Messer, Sulzbach, Germany.

Metabolite pools

Volatile fatty acids and ethanol were measured by gas chromatography using an FFAP column (25 m × 0.32 mm × 0.5 μm; J&W Scientific, Folsom, CA, USA) and a flame ionization detector; the injector and detector temperatures were 240°C. Initially, the column temperature was 80°C for 1 min, then increased to 120°C at 20°C min^{-1}, 205°C at 6.1°C min^{-1}, and then was maintained at 205°C for 2 min. The carrier gas was nitrogen with a flow rate of 2 ml min^{-1}. Samples were prepared as described in Tholen and Brune (2000).

For other fermentation products, guts were homogenized in 90 μl ice-cold Millipore water and centrifuged (10 min, 20 000 *g*, 4°C). The supernatant was acidified with an H_2SO_4 solution (2 μl, 5 M) and then centrifuged; the supernatant was analyzed by high-performance liquid chromatography (HPLC) on a Grom Resin ZH column (250 × 8 mm i.d., Grom, Rottenburg, Germany) at 60°C, using a mobile phase of 5 mM H_2SO_4 (0.6 ml min^{-1}) and a refractive index detector.

For determination of the total CO_2 pool (CO_2(aq), H_2CO_3, HCO_3^- and CO_3^{2-}), hindguts were homogenized in 10 mM NaOH (70 μl) and centrifuged as described above. The supernatant was analyzed by flow injection as described by Hall and Aller (1992).

Carbon flow measurements

Metabolite fluxes were measured by microinjection of ^{14}C-labeled compounds as described by Brune and Pester (2005). Briefly, 50–100 nl of ^{14}C-labeled compound was injected into dissected hindguts embedded in agarose-solidified insect Ringer's solution. To ensure correct rate determinations, the pool sizes of the respective substrates in embedded hindguts were determined at the time point of injection. The increase in pool sizes by the injected label was 1–7% in the case of CO_2, 4–30% in the case of lactate and 40% in the case of formate. The turnover of the injected compound and the formation of its products were monitored over time by HPLC (see above) and online radioactivity detection (Ramona 2000, Raytest, Straubenhardt, Germany). Radiolabeled CO_2 was separated by flow injection and measured by liquid scintillation counting or, in the case of ^{14}C-carbonate injection, determined from the total recovery of radioactivity minus the sum of radioactivity in the other metabolites. Recovery of total radioactivity in the samples was measured by liquid scintillation counting.

Rates of substrate turnover and product formation were determined using the label dilution model, which is briefly described in the following. The turnover rate of injected compounds (R_S) was calculated using the following equations:

$$X_S(t) = X_0 \cdot e^{\mu \cdot t} \quad (1)$$

$$R_S = \mu \cdot N \quad (2)$$

where X_S is the radioactivity in the substrate pool, X_0 the radioactivity of the injected substrate at the time of injection, μ is the turnover rate constant, N is the substrate pool and t is the time. The formation rate of products (R_P) was calculated using

$$X_P(t) = \frac{R_P \cdot A_0}{\mu}(e^{\mu \cdot t} - 1) \quad (3)$$

where A_0 is the specific radioactivity of the substrate pool at the time of injection. To ensure exact rate determinations, N and the respiratory CO_2 emission were determined separately for each batch of termites.

Radiochemicals with the following specific and volume activities were used: $Na_2^{14}CO_3$, 1.9 MBq μmol^{-1} and 24.4 MBq ml^{-1} (Moravek Biochemicals, Brea, CA, USA); [^{14}C]Na formate, 2.2MBq μmol^{-1} and 7.4 MBq ml^{-1} (GE Healthcare, Little Chalfont, Great Britain); L-[U-^{14}C]Na lactate, 5.6 MBq μmol^{-1} and 6.2 MBq ml^{-1} (ARC, St Louis, MO, USA); [2,3-^{14}C] succinic acid, 3.1 MBq μmol^{-1} and 3.7 MBq ml^{-1} (ARC); L-[U-^{14}C]malic acid, 1.9 MBq μmol^{-1} and 7.4 MBq ml^{-1} (GE Healthcare); [2-^{14}C]Na propionate, 2.0 MBq μmol^{-1} and 37.0 MBq ml^{-1} (Moravek Biochemicals); and [2-^{14}C]Na acetate, 2.1 MBq μmol^{-1} and 7.4 MBq ml^{-1} (ARC). Radiochemical purity of all radiochemicals was >95%.

Parameters for diffusion models

Calculations of net hydrogen production rates are based on an average gut length of 1.5 mm for *R.*

santonensis and 2.8 mm for *Z. nevadensis*, the diffusion coefficient (D) of H_2 in pure water at 21°C (3.81×10^{-5} cm^2 s^{-1}; Gertz and Loeschcke, 1954) and a porosity (ϕ) of 0.5, which takes into account that termite hindguts are tightly packed with protozoa filled to approximately 50% with ingested wood particles. Similar porosities have been determined for densely packed biofilms (Revsbech, 1989).

Hydrogen emission rates of embedded guts were calculated from the hydrogen concentration profiles in the surrounding agarose, using a diffusion model for systems with circular symmetry (Koch, 1990), D of H_2 in water and $\phi = 1$, which was found applicable for agar concentrations up to 2% and over a wide range of salinity values (Revsbech, 1989).

Results

Characteristics of model termites

Reticulitermes santonensis was the smallest of the termites studied, followed by *Cryptotermes secundus* and *Zootermopsis nevadensis*, as indicated by their fresh weight and the volume of their hindgut, which takes up the major part of the abdomen (Table 1). All three termites showed a low apparent redox potential in the center of the hindgut (Table 1), which was previously shown to correlate with anoxia (Ebert and Brune, 1997). The metabolite pools in the hindgut consisted of typical fermentation products from carbohydrates, and the overall composition was similar in all three termite species, with acetate and CO_2 being the major metabolites (Table 2). The CO_2 emission rate of all three termite species was in the same range when normalized to the respective fresh weight (Table 1). The respiratory electron flow was calculated from the CO_2 emission rates (assuming the average oxidation state of wood polysaccharides to be 0; Odelson and Breznak, 1983), corrected for the H_2 and CH_4 emission rates of the same termites (see below).

Hydrogen accumulation and emission

Hydrogen microsensor measurements revealed pronounced differences in hydrogen partial pressure in the hindguts of the three species. The highest values were obtained for the large *Z. nevadensis*, often nearing saturation at the center of the hindgut paunch, the gut region with the largest diameter (Table 1). Also in the paunch of *R. santonensis*, the smallest of the three termites, H_2 accumulated to substantial amounts, whereas hydrogen partial pressures in the paunch of the slightly larger *C. secundus* were much lower and averaged 1 kPa. Axial profiles documented that H_2 accumulated mainly in the enlarged hindgut paunch of all three termite species, whereas the relatively narrow and tubular-like midgut and—with the exception of the large *Z. nevadensis*—also the colon and rectum showed little or no accumulation of H_2 (Figure 1). Radial profiles through the paunch of *R. santonensis* and *Z. nevadensis* showed a bell-shaped distribution of H_2 with the maximum concentration in the center of the paunch, and a decrease towards the gut wall (Figure 1). Similarly shaped profiles were obtained also for *C. secundus*, but profiles were much more asymmetric and less reproducible than with the other species.

These results were in agreement with the emission of H_2 from living termites, which was only detected for *R. santonensis* and *Z. nevadensis* (Table 3). In both termite species, however, hydrogen emission accounted for less than 0.1% of the respiratory electron flow. Similar results were obtained in previous studies with other lower termites (Ebert and Brune, 1997; Nunes *et al.*, 1997). When the headspace over *R. santonensis* and *Z. nevadensis* was exchanged with N_2, hydrogen emission increased immediately, albeit only slightly when compared to the respiratory electron flow (Figure 2).

Methanogenesis

Methane emission was detected only for *R. santonensis* and *Z. nevadensis* (Table 3). This is in agreement with the lack of coenzyme F_{420}-autofluorescent cells in hindgut preparations of *C. secundus*, which indicated the absence of methanogenic archaea. In *R. santonensis*, autofluorescent cells were located exclusively at the microoxic hindgut wall, patchily distributed in microcolonies, which is in agreement with previous reports on *Reticulitermes*

Table 1 Characteristics of the termites investigated in this study

Termite	*Family*	*Fresh weight (mg)*	*Hindgut volume (µl)*	*CO_2 emission (µmol (g fresh wt)$^{-1}$ h^{-1})*	*Hindgut maximum H_2 partial pressure (kPa)*[a]	*Hindgut apparent redox potential (mV)*[b]
R. santonensis	Rhinotermitidae	2.0±0.1	0.4±0.1	15.9±0.4	29.8±14.6	−290 to −260
Z. nevadensis	Termopsidae	28.4±5.6	7.5±1.1	30.8±5.7	72.2±28.5	−240 to −210
C. secundus	Kalotermitidae	2.8±0.4	2.2±0.6	23.9±0.9	1.3±1.1	−130 to −80

Values are averages (±s.d.) of at least four independent measurements.
[a]Values were taken at the center of the hindgut paunch.
[b]Values were rounded to the nearest factor of 10.

Table 2 Metabolites detected in total hindgut extracts of freshly dissected worker termites

Termite	*Pool size (nmol hindgut^{-1})*[a]									
	Glucose	*Malate*	*Succinate*	*Butyrate*	*Propionate*	*Lactate*	*Acetate*	*Ethanol*	*Formate*	*CO_2*
R. santonensis	2.4±0.8	0.1±0.0	0.4±0.1	0.1±0.0[b]	0.3±0.1	0.4±0.0	11.3±2.6	0.8±0.6	1.7±0.6	10.7±0.7
Z. nevadensis[c]	6.0±1.6	0.3±0.2	10.3±4.8	<0.02	5.1±2.4[b]	2.1±1.2	53.5±13.5[b]	10.4±1.8[b]	26.4±4.8	142.5±33.8[b]
C. secundus[d]	0.1±0.1	n.m.[e]	0.2±0.1	0.5[f]	1.0[f]	4.0±1.8	38.5[f]	0.8[f]	1.1±0.8	28.3±2.6[b]

[a]At least three independent measurements were used for determinations of averages and standard deviations. The detection limit was 0.02 nmol.
[b]Mean and range of two independent measurements.
[c]Isovalerate was detected in two independent measurements (10 nmol hindgut^{-1}, mean).
[d]Isovalerate was detected in two independent measurements (0.1 nmol hindgut^{-1}, mean).
[e]Not measured.
[f]Single measurement.

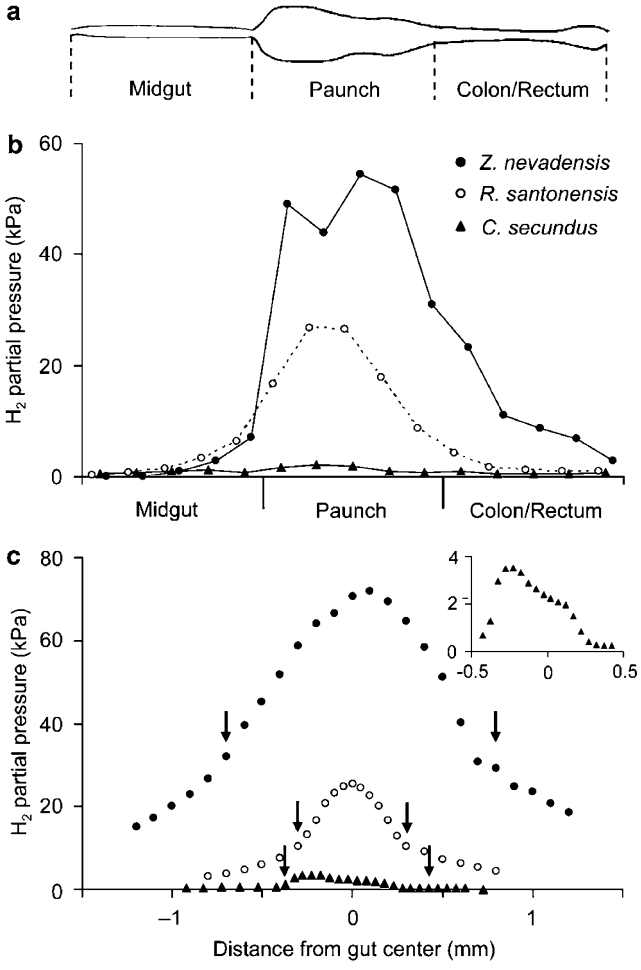

Figure 1 Axial and radial hydrogen concentration profiles of agarose-embedded guts of *Zootermopsis nevadensis*, *Reticulitermes santonensis*, and *Cryptotermes secundus*. (**a**) Schematic diagram of the gut of lower termites, showing the midgut and the different hindgut regions (paunch, colon, and rectum). (**b**) Typical axial profiles of the three termite species, normalized using five cardinal points per gut section to account for different gut lengths. (**c**) Typical radial profiles across the hindgut paunch of the three termite species. Arrows indicate the position of the hindgut wall. The inset shows the enlarged radial profile of *C. secundus* from gut wall to gut wall.

flavipes (Leadbetter and Breznak, 1996). Two morphotypes were distinguishable: rod-shaped cells of 1 μm length, resembling *Methanobrevibacter cuticularis* (Leadbetter and Breznak, 1996), and coccoid cells of 0.2 μm in diameter. In *Z. nevadensis*, the situation was completely different and resembled that previously described for *Zootermopsis angusticollis* (Lee *et al.*, 1987; Messer and Lee, 1989). Here, autofluorescent cells were located mainly within the cytoplasm of the gut flagellates *Trichomitopsis termopsidis, Hexamastix termopsidis* and *Tricercomitus termopsidis*. Only occasionally were autofluorescent cells detected also at the hindgut wall, but at much lower densities than in *R. santonensis*.

Since methane is not oxidized in termites (Pester *et al.*, 2007), methanogenesis in the hindgut is equal to the methane emission rate of the termite, constituting about 4% of the respiratory electron flow in both *R. santonensis* and *Z. nevadensis* (Table 3). Supplementation of H_2 to the atmosphere surrounding the termites led to a fivefold stimulation of methane emission in *R. santonensis* (Figure 2), which indicated that the methanogens at the hindgut wall are hydrogen-limited. In *Z. nevadensis*, this effect was much less pronounced, probably because the protozoa-associated methanogens in this termite are located in a gut region with higher hydrogen concentrations. In agreement with microscopy observations, *C. secundus* did not emit any CH_4 also in an atmosphere supplemented with H_2 (Figure 2).

Acetogenesis from CO_2

Microinjection of ^{14}C-labeled carbonate into intact termite hindguts was used to follow the fate of total CO_2 (sum of CO_2(aq), H_2CO_3, HCO_3^- and CO_3^{2-}). The injected label (1–7% of the pool size) did not substantially increase the CO_2 pool of the hindgut. In all three termite species, acetate was the only product detected (Figure 3). The depletion rate of labeled CO_2 and formation rate of labeled acetate decreased over time, reflecting the continuous decrease in the specific radioactivity (radioactivity per molarity) of the CO_2 pool. The data were in agreement with the label dilution model (Brune and Pester, 2005). Resulting rates of acetogenesis from CO_2 (Table 3) corresponded to 18% (±7%) and 22% (±3%) of the respiratory electron flow in

Table 3 Processes involved in hydrogen turnover in the hindgut

Termite	*Rate (μmol C (g fresh wt)$^{-1}$ h^{-1})*		*Rate (μmol H_2 (g fresh wt)$^{-1}$ h^{-1})*	
	Reductive acetogenesis[a]	*CH_4 emission*[b]	*H_2 emission*[b]	*Sum of H_2 turnover*[c]
R. santonensis	2.93±1.11	0.29±0.01	0.05±0.01[d]	7.1
Z. nevadensis	6.88±1.08	0.63±0.11	0.08±0.00	16.4
C. secundus	6.31±1.01	0.00±0.00	0.00±0.00[e]	12.6

Values are averages (±s.d.) of at least three independent measurements.
[a]Calculated from data in Figure 3; based on the CO_2 pool of embedded hindguts of the particular batch of termites at the time point of injection (*R. santonensis*, 8.4 nmol; *Z. nevadensis*, 120 nmol; *C. secundus*, 14.0 nmol) and the assumption that both carbon atoms of the acetate molecule stem from CO_2 (Breznak and Switzer, 1986).
[b]Emission from living termites.
[c]Sum of hydrogen-utilizing processes and hydrogen emission, assuming that reductive acetogenesis and methanogenesis are completely hydrogen-dependent. For details, see Discussion. Rates correspond to 14.5 (*R. santonensis*), 464 (*Z. nevadensis*), and 35.3 (*C. secundus*) nmol H_2 termite^{-1} h^{-1}.
[d]The CO_2 emission rate of the termite batch used for H_2 emission measurements was above average (Table 1): 24.0±0.2 μmol C (g fresh wt)$^{-1}$ h^{-1}.
[e]Two independent measurements. The detection limit was 0.5 nmol H_2 (g fresh wt)$^{-1}$ h^{-1} for 12 termites per vial.

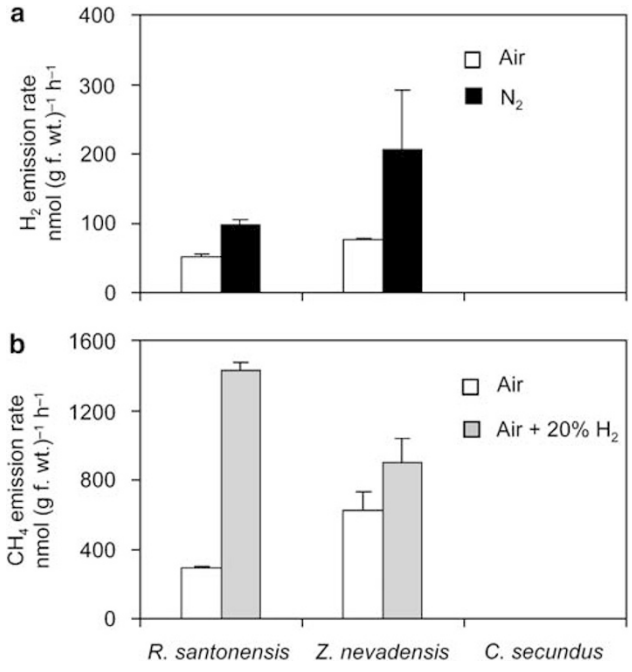

Figure 2 Emission of H_2 (**a**) and CH_4 (**b**) from living termites incubated under different atmospheres. Bars represent averages of at least three independent measurements; standard deviations are indicated. The absence of hydrogen emission from *C. secundus* was measured only under air (two independent measurements).

R. santonensis and *Z. nevadensis*, and 26% (±4%) in *C. secundus*.

In all termite species, the turnover rate of CO_2 was higher than the formation rate of acetate, which is mainly due to the inevitable diffusion of CO_2 from the gut into the surrounding agarose. An additional, albeit minor CO_2-consuming process in *R. santonensis* and *Z. nevadensis* is methanogenesis (see above).

Lactate and formate turnover

Injection of labeled lactate into hindguts of *R. santonensis* resulted in substrate depletion and product formation curves that again corresponded well to the label dilution model (Figure 4). Two-thirds of the carbon atoms of lactate were recovered as acetate, whereas the remaining carbon atoms were detected in the CO_2 pool (Table 4), which indicated that lactate is converted to acetate and CO_2 in an equimolar ratio. Lactate turnover corresponded to 10% of the respiratory electron flow.

Injection of labeled lactate into hindguts of *C. secundus* produced similar results (Figure 4). Although the depletion rate of labeled lactate and the formation rates of the labeled products (acetate and CO_2) were lower than in *R. santonensis*, lactate turnover rates (11% of the respiratory electron flow) were similar in the two termite species. This is due to the larger lactate pool in *C. secundus* (Table 2). The recovery of labeled carbon in the acetate pool (55% of the injected label) and a low recovery of label in the CO_2 pool (10% of the injected label), together with a similar gap in the total recovery of radioactivity, indicated the loss of a gaseous product, probably additional CO_2 (Table 4).

Since H_2 accumulated only to moderate amounts in the hindgut of *C. secundus*, we tested formate as an alternative substrate of reductive acetogenesis. Upon injection into hindguts, labeled formate was rapidly turned over to acetate and CO_2 (Figure 4). Although the label entering the acetate pool behaved as predicted by the label dilution model, this was not the case for formate. The divergence from the model was even more pronounced in the case of the CO_2 pool, where the label was stable throughout the incubation period. The criteria of the model are apparently not fulfilled, possibly because of pool compartmentation and/or non-steady-state conditions. To minimize artifacts and remain as close as possible to *in vivo* conditions, we used only the first time interval (2 min after injection) for the calculations. During this time, 30% of the formate label was recovered in the acetate pool and 50% was recovered in the CO_2 pool, documenting that at least half of the formate was oxidized to CO_2. The total formate turnover rate corresponded to 5% of the respiratory electron flow.

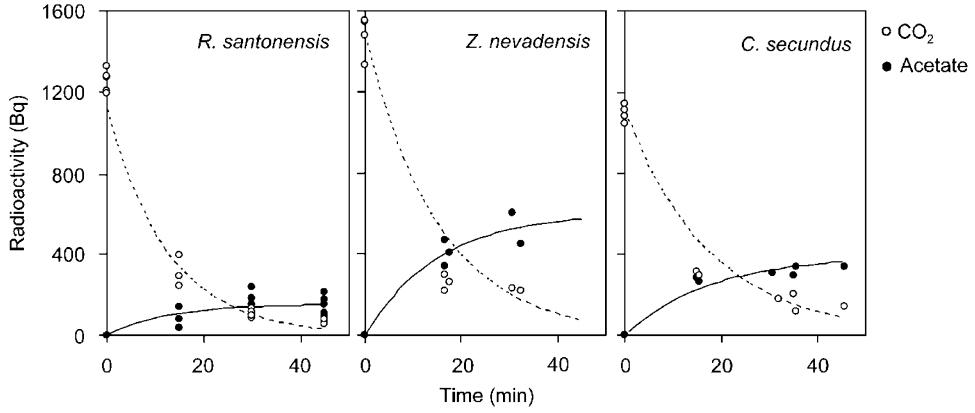

Figure 3 Time course of label distribution of total CO_2 and acetate after microinjection of ^{14}C-carbonate into the paunch of agarose-embedded guts of *Reticulitermes santonensis*, *Zootermopsis nevadensis*, and *Cryptotermes secundus*. Each value represents an injection into a separate gut. Expected time curves of substrate depletion (dotted line) and product formation (solid line) were plotted with the measured values.

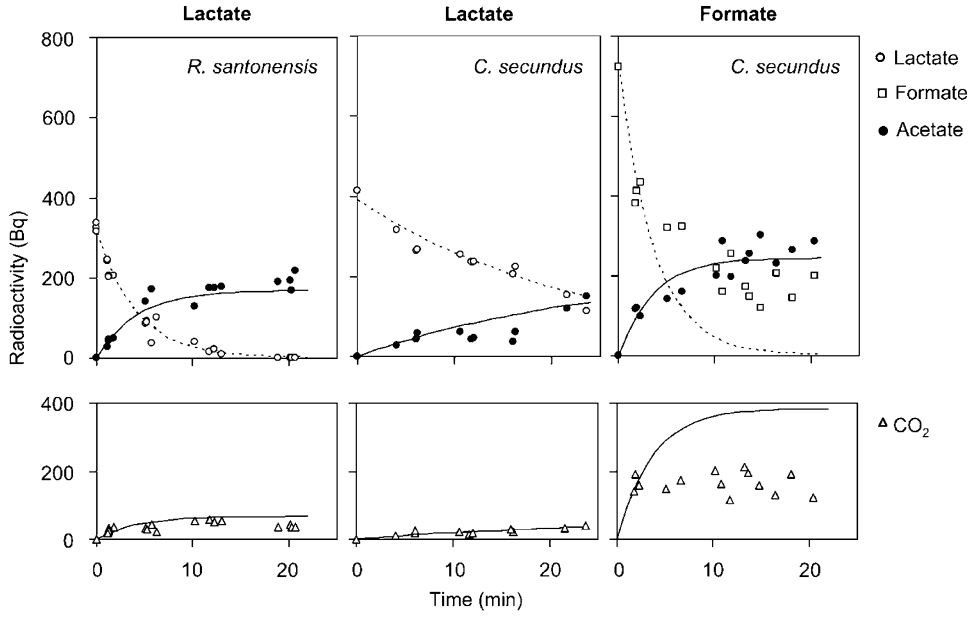

Figure 4 Time course of label distribution of different metabolites after microinjection of [U-^{14}C]lactate and ^{14}C-formate into the paunch of agarose-embedded guts of *Reticulitermes santonensis* and *Cryptotermes secundus*. Each value represents an injection into a separate gut. Expected time curves of substrate depletion (dotted line) and product formation (solid line) were plotted with the measured values.

The proportion of label in the methyl and carbonyl groups of acetate is uncertain. Theoretically, formate label enters the methyl branch of reductive acetogenesis, where it is reduced, yielding the methyl group of acetate. In addition, the formate label is oxidized to CO_2. Any label in the CO_2 pool may subsequently enter the carbonyl branch of reductive acetogenesis, where it is reduced, yielding the carbonyl group of acetate (Drake *et al.*, 2006). For the calculation of the highest possible acetate formation rates from formate, we assumed that all formate label is present in the methyl group of acetate, resulting in a ratio of one formate used per acetate formed. The respective carbon fluxes are given in Table 4. Actual rates of acetogenesis from formate will be lower, since formate label contributed also to the CO_2 pool. As a consequence, an uncertain amount of label will inevitably end up in the carbonyl group of acetate, resulting in more than one formate used per acetate formed.

Radial distribution of net hydrogen production

We addressed the reason for the bell-shaped distribution of hydrogen in the hindgut by mathematical modeling. Regression analysis revealed that the distribution of hydrogen concentration c over the gut radius r is best approximated by a fourth-order parabola:

$$c_{H_2}(r) = \alpha \cdot r^4 + \beta \cdot r^3 + \gamma \cdot r^2 + \delta \cdot r + \varepsilon \qquad (4)$$

Viewing the hindgut as a cylinder allows the situation to be reduced to a two-dimensional circular system with radius r and length l (Koch,

Table 4 Turnover rates of lactate and formate, and formation rates of their respective products in the hindgut of *R. santonensis* and *C. secundus*

Metabolite		*Rate (μmol C (g fresh wt)$^{-1}$ h^{-1})*[a]	
Injected	*Produced*	R. santonensis	C. secundus
Lactate		−2.40[b]	−2.53
	Acetate	1.61	1.38
	CO_2	0.64	0.24
Formate		−0.63[c]	−2.53[d]
	Acetate	0.00	1.22[d,e]
	CO_2	0.48	1.87[d]

Rates were determined by microinjection of ^{14}C-labeled metabolites into agarose-embedded hindguts.
[a]Calculated from data in Figure 4; based on the lactate pool (*R. santonensis*, 0.2 nmol; *C. secundus*, 1.9 nmol) and formate pool (*C. secundus*, 0.8 nmol) of embedded hindguts of the particular batch of termites at the time point of injection.
[b]The CO_2 emission rate of this termite batch was above average (Table 1): 24.0 ± 0.2 μmol C (g fresh wt)$^{-1}$ h^{-1}.
[c]Data from Tholen and Brune (2000) obtained for *R. flavipes*, a species synonymous to *R. santonensis* (Austin *et al*., 2005).
[d]Rates were calculated using only data points obtained within the first 2 min after injection.
[e]Assuming that only the methyl group stemmed from formate.

1990). This cylinder was partitioned into infinitely many radial sections with a surface area A, which increases as a function of r (equation (5)). Using Fick's first law of diffusion (equation (6)) and substituting dc/dr with the first derivative of equation (4), the diffusion flux J at a given diffusion coefficient (D) and porosity ϕ can be determined for every radial section (equation (7)).

$$A = 2 \cdot \pi \cdot l \cdot r \tag{5}$$

$$J = -\phi \cdot D \cdot A \cdot \frac{dc}{dr} \tag{6}$$

$$J(r) = -\phi \cdot D \cdot 2 \cdot \pi \cdot l \cdot r \cdot \frac{dc}{dr} \tag{7}$$

The slope of the hydrogen concentration curve (Figure 1) documents the diffusion flux changes over the gut radius. Flux changes (dJ/dr) can be described by extending Fick's second law of diffusion by the inclusion of a production (P) and a consumption (C) term (Revsbech and Jørgensen, 1986). Excluding a net flux along the length axis of the gut allows this equation to be used in its one-dimensional form.

$$\frac{dJ}{dr} = -A \cdot \frac{dc}{dt} + \frac{P - C}{dr} \tag{8}$$

At steady state, the concentration in any radial section does not change over time ($dc/dt = 0$). It follows that the difference of hydrogen flux into and out of any cylindrical layer of the thickness dr is equal to the difference of hydrogen production (P) and hydrogen consumption (C) in that same layer. The resulting net hydrogen production rate (R) is positive if that layer is a hydrogen source and negative if that layer is a hydrogen sink:

$$dJ_{dr} = P - C = R \tag{9}$$

Normalizing to the volume, the volume-specific net hydrogen production rate R_V in a cylindrical layer of any definite thickness (with outer radius r_m and inner radius r_n) can be calculated:

$$R_V = \frac{P - C}{V} = \frac{J(r_m) - J(r_n)}{2 \cdot \pi \cdot l \cdot (r_m^2 - r_n^2)} \tag{10}$$

The distribution of R and R_V over the gut radius was determined using the hydrogen profiles obtained for the individual termite species (Figure 1). In *R. santonensis*, R continuously increased with the gut radius in the central gut region, which correlates with the increasing volume of the cylindrical sections (Figure 5a). Toward the gut periphery, R decreased again until it eventually became negative in the gut periphery. A similar situation was observed for *Z. nevadensis*, although the absolute values of R were higher owing to the larger gut radius of this termite (Figure 5a).

In contrast to R, the volume-corrected rates (R_V) were relatively constant in the gut center (Figure 5b). R_V was significantly higher in *R. santonensis* (55–131 nmol H_2 h^{-1} mm^{-3}, $n = 3$) than in *Z. nevadensis* (22–27 nmol H_2 h^{-1} mm^{-3}, $n = 2$), which indicated that the higher hydrogen concentrations in the gut of *Z. nevadensis* are merely a consequence of the larger gut radius. For both termites, R_V decreased continuously towards the gut periphery.

The experimental data for *C. secundus* could not be fitted by a regression curve according to equation (4), because the distribution of H_2 was never completely symmetric. Nevertheless, the principles laid out above apply also for *C. secundus*. The much lower hydrogen concentrations throughout the gut signify that dJ/dr (equations (7 and 8)) and therefore also R and R_V were much smaller over the gut radius in *C. secundus* when compared to the similar-sized *R. santonensis*. It follows that differences in the rates of hydrogen production and hydrogen consumption were much smaller throughout the gut.

Figure 5 documents that the sum of R of the individual layers is not balanced over the gut. This discrepancy is in agreement with the hydrogen emission rates from embedded guts (6–14 nmol h^{-1} for *R. santonensis* and 32–34 nmol h^{-1} for *Z. nevadensis*), which are considerably higher than those of the living termite (0.2 and 2.4 nmol h^{-1}, respectively). Possible explanations may be that the embedded gut is oxygen limited or that the wall-associated microbiota was damaged by the embedding procedure. Moreover, the rates for R and R_V may differ slightly from the actual rates because values for D and ϕ were not determined experimentally (for details, see Materials and methods).

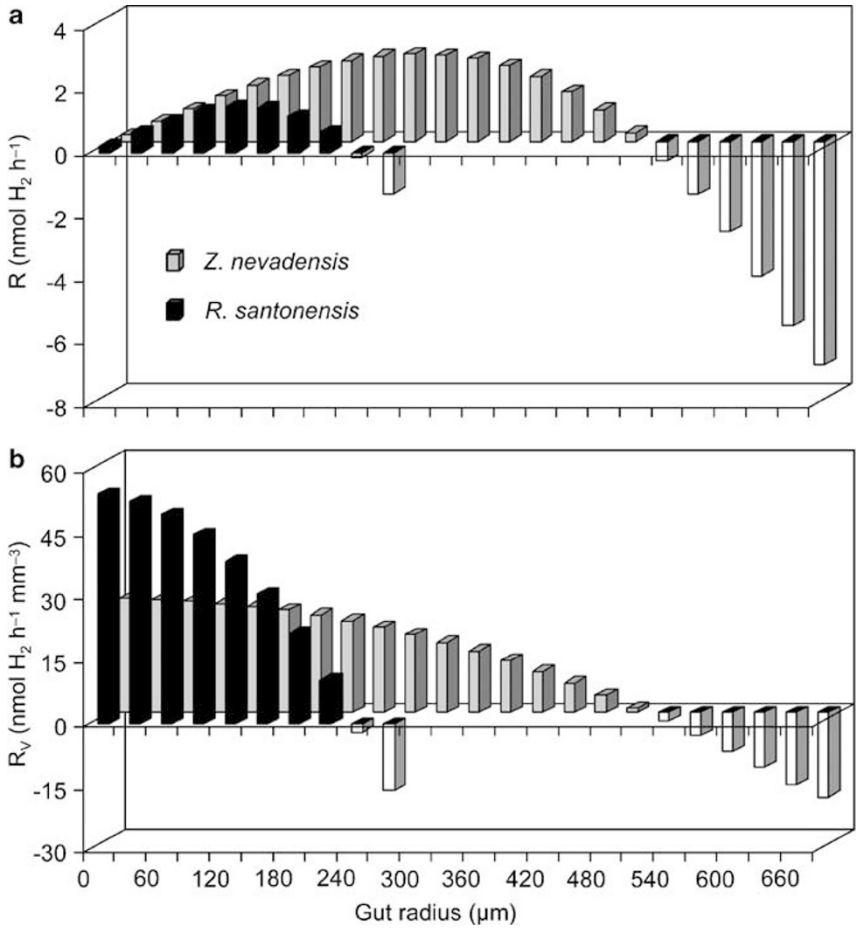

Figure 5 Typical distribution of the net hydrogen production rate R (**a**) and the volume-specific net hydrogen production rate R_V (**b**) over the gut radius of the small *R. santonensis* and the large *Z. nevadensis*. Rates were determined for cylindrical gut layers of 30 μm thickness, which corresponds to the diameter of the *Trichonympha* cells (30–40 μm) that make up the bulk of the hindgut volume in *R. santonensis*. Negative values of R and R_V are depicted in white.

Discussion

Over the course of several decades, the concept of molecular hydrogen as a key intermediate of lignocellulose degradation in lower termites has developed to an entirely plausible and generally accepted hypothesis (reviewed by Breznak, 1994, 2000; Brune, 2006). However, measurements of hydrogen gradients and metabolite fluxes in intact guts of *Reticulitermes flavipes* (Ebert and Brune, 1997; Tholen and Brune, 2000) had indicated that several important issues remained to be addressed: a reliable estimation of hydrogen turnover with respect to other relevant processes, the explanation of its radial dynamics, and clarification whether the concept is generally applicable to lower termites.

Processes involved in hydrogen turnover

In all lower termites investigated to date, only a small fraction of reducing equivalents released during lignocellulose degradation escapes the system directly by H_2 emission (Odelson and Breznak, 1983; Ebert and Brune, 1997; Nunes *et al.*, 1997; Sugimoto *et al.*, 1998; this study), indicating that most of the H_2 produced is also consumed within the hindgut. Even if one takes into account that methanogenesis in termite guts is completely hydrogen driven, as suggested by the results of numerous studies (Breznak and Switzer, 1986; Leadbetter and Breznak, 1996; Leadbetter *et al.*, 1998; Ohkuma *et al.*, 1999; Shinzato *et al.*, 1999; Tokura *et al.*, 2000), methanogenesis constitutes only a minor hydrogen sink (Odelson and Breznak, 1983; Brauman *et al.*, 1992, this study).

By contrast, the *in situ* flux measurements obtained in this study document that CO_2-reductive acetogenesis is the dominant hydrogen sink in the termite species investigated. This is the final experimental proof of John Breznak's hypothesis that CO_2-reductive acetogenesis is the major hydrogen sink at least in lower termites, as postulated previously on the basis of a large data set of potential rates determined in gut homogenates (Breznak and Switzer, 1986; Brauman *et al.*, 1992) and the high hydrogen emission rate of *Reticulitermes flavipes*

after treatment with antibacterial drugs (Odelson and Breznak, 1983).

The *in situ* rates of reductive acetogenesis obtained in this study by microinjection of ^{14}C-carbonate are similar to the potential rates of hydrogen-dependent reductive acetogenesis obtained previously in gut homogenates of the same termite species (4–12 μmol C (g termite fresh weight)$^{-1}$ h^{-1}; Pester and Brune, 2006). The potential contribution of formate and lactate to reductive acetogenesis was only minor (see below), making H_2 the most important electron donor of reductive acetogenesis. Surprisingly, reductive acetogenesis was the dominant hydrogen sink not only in *R. santonensis* and *Z. nevadensis*, the species with high intestinal hydrogen concentrations, but also in *C. secundus*, which accumulated H_2 only to moderate amounts. Evidently, the hydrogen pool is subject to a high turnover in all three species, irrespective of the degree of hydrogen accumulation.

The hydrogen turnover rates reported in this study are based on the assumption that reductive acetogenesis is completely hydrogen-driven. In principle, electron donors other than H_2 may contribute to reductive acetogenesis from CO_2. The prime candidates are lactate and formate, which are readily turned over in the hindgut of *Reticulitermes flavipes* (Tholen and Brune, 2000) and are known to be used by homoacetogens (Drake *et al.*, 2006). To address this possibility, we compared lactate and formate turnover in *R. santonensis* and *C. secundus*, the two termite species with a similar size but completely different degrees of hydrogen accumulation.

In the hydrogen-accumulating *R. santonensis*, lactate was converted into acetate and CO_2 at an equimolar ratio, clearly showing the absence of a complete homoacetogenic turnover. The same was observed with *R. flavipes* previously (Tholen and Brune, 2000), a species considered synonymous to *R. santonensis* (Austin *et al.*, 2005). Similar results were also obtained with *C. secundus*, the termite species that accumulated only moderate amounts of H_2. Even if one assumes that lactate is converted by two separate processes, that is, aerobic oxidation to CO_2 and homoacetogenesis, the reduction of CO_2 by intermediately formed reducing equivalents would not surpass 2% of the respiratory electron flow in both termites. Moreover, results obtained with *R. flavipes* indicate that not homoacetogenic but rather propionigenic bacteria are responsible for lactate turnover (Tholen and Brune, 2000).

Formate metabolism differs considerably between the two species. In *R. flavipes*, injected formate is oxidized exclusively to CO_2, which accumulates over time (Tholen and Brune, 2000). In *C. secundus*, however, one-third of the injected formate label appeared in the acetate pool already 2 min after injection, indicating a direct contribution of formate to reductive acetogenesis. It is puzzling why the formate label entering the CO_2 pool remained constant over time; this may indicate the presence of a second, possibly intracellular, CO_2 pool that is turned over faster than it can exchange with the large CO_2 pool of the whole hindgut. It is not clear whether the reducing equivalents of formate oxidation are used for reductive acetogenesis, oxygen reduction or other processes. In any case, maximal contribution of these reducing equivalents to the respiratory electron flow would be 2–5% (Tholen and Brune, 2000; this study), which makes their possible contribution to reductive acetogenesis small.

Additional potential substrates that might drive reductive acetogenesis from CO_2 are carbohydrates resulting from cellulose and hemicellulose hydrolysis. Although the large population of anaerobic protozoa, which form the bulk of the biovolume in the hindgut of lower termites, are considered the major agents of polysaccharide degradation (Breznak, 2000; Brune and Stingl, 2005), cellobiose, glucose and xylose have been identified as potential substrates of termite gut homoacetogens (Breznak, 1994; Graber *et al.*, 2004). However, it is not clear whether (or to which extent) monomeric or oligomeric hydrolysis products are released by the protozoa and subsequently fermented by homoacetogens. Moreover, a substantial contribution of sugar-fermenting homoacetogens to intestinal hydrogen pools seems unlikely in view of the fact that even in the case of *C. secundus*, the hydrogen concentrations in the gut center were on average more than one order of magnitude higher than the accumulation of free H_2 during homoacetogenic conversion of sugars by termite gut homoacetogens (490−830 ppmv H_2; Cord-Ruwisch *et al.*, 1988; Graber and Breznak, 2004) and at least 2−3 times higher when compared to hydrogen thresholds of homoacetogens in general (362–4660 ppmv H_2; Drake *et al.*, 2006).

Flux analysis of hydrogen metabolism

We compiled the results of the individual experiments for a balance analysis of hydrogen-producing and hydrogen-consuming processes (Figure 6). The model assumes that wood polysaccharides are fermented either to lactate (Tholen and Brune, 2000) or to acetate, CO_2 and H_2 (Odelson and Breznak, 1983) (equation (11)), with formate being equivalent to $CO_2 + H_2$.

$$\langle C_6H_{12}O_6\rangle + 2H_2O \rightarrow 2CH_3COOH + 2CO_2 + 4H_2 \quad (11)$$

In the hydrogen-accumulating *R. santonensis*, the lactate turnover rate contributed 10% to the respiratory electron flow. Presumably, lactate was subsequently oxidized to acetate and CO_2 in the microoxic periphery of the hindgut, with the electrons being transferred to molecular oxygen (Tholen and Brune, 2000). This leaves 90% of the polysaccharides to be fermented, according to equation (11), with the

influx into the hydrogen pool (28% of the respiratory electron flow) diminished by the formation of formate. This estimated influx was slightly higher than the efflux from the hydrogen pool (22% of the respiratory electron flow), which is the sum of reductive acetogenesis, methanogenesis and hydrogen emission. In *Z. nevadensis*, which also accumulates H_2 to high concentrations, the sum of the hydrogen-consuming processes resulted in a similar efflux rate (26% of the respiratory electron flow).

Also in *C. secundus*, the termite that accumulates only moderate amounts of H_2, 11% of the respiratory electron flow proceeded through lactate, which was probably oxidized in the microoxic gut periphery as well. This leaves 89% of the electrons in the remaining polysaccharides to be converted to acetate, H_2 and formate. Although the respiratory electron flow through formate was considerably higher, the estimated influx into the hydrogen pool (25% of the respiratory electron flow) was in the same range as in *R. santonensis*. The efflux rate, which was equal to the rate of reductive acetogenesis in *C. secundus*, was slightly higher (26% of the respiratory electron flow) than the estimated influx rate, which indicates that at least part of the reducing equivalents from formate were used in reductive acetogenesis.

The slight imbalances observed between the influx and efflux of the hydrogen pool are actually not unexpected. It is likely that some of the H_2 is used in oxygen reduction (Leadbetter and Breznak, 1996; Boga and Brune, 2003; Graber and Breznak, 2004; Seedorf *et al.*, 2004). In addition, the model does not account for alternative fermentation pathways, for example, malate and succinate formation, or for the direct uptake of polysaccharide monomers in the midgut. Also, a contribution of sulfate-reducing bacteria to hydrogen turnover cannot be ruled out, especially since *Desulfovibrio* spp have been repeatedly isolated from the termite hindgut (Brauman *et al.*, 1990; Trinkerl *et al.*, 1990; Kuhnigk *et al.*, 1996; Fröhlich *et al.*, 1999). However, molecular studies using cloning and terminal restriction fragment length polymorphism (T-RFLP) analysis of 16S rRNA genes suggest very low population densities of this metabolic group in

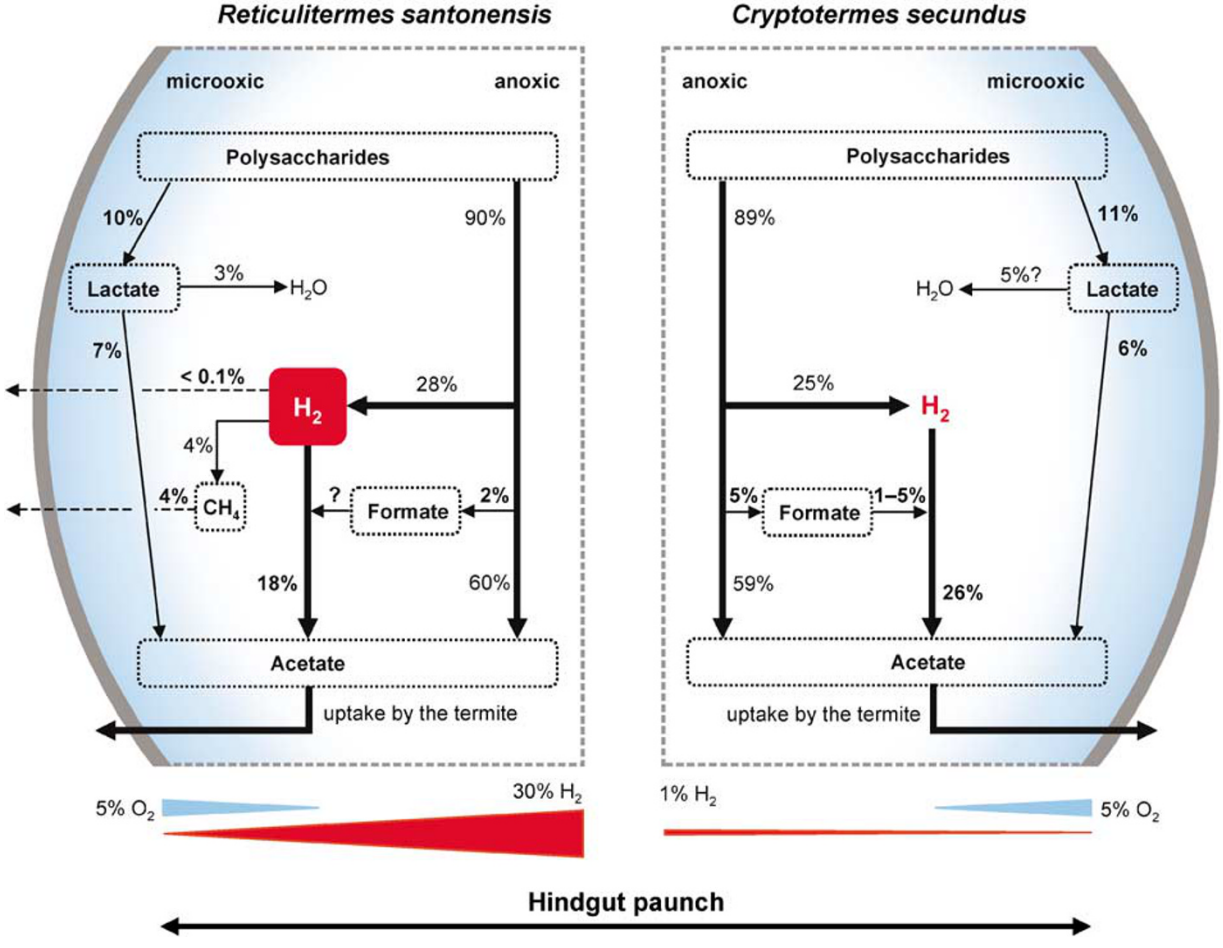

Figure 6 Proposed model of hydrogen metabolism in *Reticulitermes santonensis* and *Cryptotermes secundus*. Values stem from turnover experiments of CO_2, formate, and lactate and emission rates of H_2 and CH_4 (Tables 3 and 4) and are based on the respiratory electron flow, calculated from the respiratory CO_2 formation (assuming the average oxidation state of wood polysaccharides to be zero; Odelson and Breznak, 1983) and the H_2 and CH_4 emission of the termites. The fluxes determined by direct measurements are given in bold. The oxygen status of the gut periphery was determined by Brune *et al.* (1995).

Reticulitermes spp (Hongoh *et al.*, 2003; Yang *et al.*, 2005). In addition, potential rates of sulfate reduction in gut homogenates of *Mastotermes darwiniensis* suggest a hydrogen turnover of $<0.1\%$ of the respiratory electron flow even when termites were fed a sulfate-enriched diet (calculated from data in Sugimoto *et al.*, 1998 and Dröge *et al.*, 2005).

It should be noted that, in contrast to this study, previous studies on *C. secundus* have reported methane emissions that were in the range of those reported for *R. santonensis* and *Z. nevadensis* when normalized to the fresh weight of the termite (Sugimoto *et al.*, 1998; Pester *et al.*, 2007). Interestingly, methane formation by *C. secundus* was accompanied by hydrogen emission (Sugimoto *et al.*, 1998). Absence and presence of methane emission among different populations of the same species have been reported also for other termites (Sugimoto *et al.*, 1998).

The results of the electron balance analysis corroborate the hypothesis that termite gut protozoa ferment wood polysaccharides to acetate, CO_2, and H_2 according to equation (11) (Hungate, 1943; Yamin, 1980, 1981; Odelson and Breznak, 1985). This means that up to 4 mol of H_2 are produced from one hexose equivalent against a high hydrogen partial pressure. Since H_2 is the only reduced fermentation product, one-half of the produced H_2 presumably originates from pyruvate oxidation via the pyruvate:ferredoxin oxidoreductase ($E_0' = -0.40$ V), a reaction that is readily coupled to hydrogenase-mediated reduction of protons to H_2 ($E_0' = -0.41$ V). The other half of the reducing equivalents presumably originates from the oxidation of glyceraldehyde 3-phosphate (GAP) to glycerate 1,3-bisphosphate (BPGA) during glycolysis. The redox potential of the BPGA/GAP + P_i couple is more positive ($E_0' = -0.35$ V) than the redox potential of the two H^+/H_2 couple ($E_0' = -0.41$ V), which makes the reduction of protons to H_2, with reducing equivalents from GAP thermodynamically unfavorable at hydrogen partial pressures >0.1 kPa (Schink, 1997). A similar situation occurs in the termite gut spirochete *T. azotonutricium* (Graber *et al.*, 2004). The observed hydrogen formation from unfavorable electron donors may be driven by reverse electron transport via a membrane-bound NADH:ferredoxin oxidoreductase (Boiangiu *et al.*, 2005), or directly by a modified complex I, as proposed for hydrogenosomes of *Trichomonas vaginalis* (Dyall *et al.*, 2004). Complex I is proposed to be related to energy-converting hydrogenases (Hedderich and Forzi, 2005).

Species-specific differences in hydrogen accumulation

It is now evident that differences in hydrogen accumulation in the termites investigated are not due to differences in intestinal hydrogen fluxes. Rather, the explanation for this apparent discrepancy may be in the spatial distribution of hydrogen-producing and hydrogen-consuming processes. Mathematical modeling indicated dynamic changes in gross hydrogen production and hydrogen consumption over the gut radius in *R. santonensis* and *Z. nevadensis*, the two termite species that accumulated high amounts of H_2. Hydrogen production dominated in the gut lumen and hydrogen consumption in the gut periphery, and higher hydrogen concentrations in *Z. nevandensis* were merely due to the larger gut radius and not higher hydrogen production rates per unit volume. In *C. secundus*, the distribution of production and consumption followed the same pattern, but in contrast to the other two termites, the rates of both processes are more balanced throughout the gut, resulting only in a moderate accumulation of H_2.

It is generally assumed that the flagellate protozoa are the major producers of H_2 in the hindgut of lower termites (Hungate, 1943; Odelson and Breznak, 1983; Breznak, 2000; Brune, 2006), with a potential bacterial contribution being possible (Graber *et al.*, 2004). Homoacetogenic spirochetes are generally considered the major H_2 consumers (Leadbetter *et al.*, 1999; Salmassi and Leadbetter, 2003; Pester and Brune, 2006; Ottesen *et al.*, 2006). Since the protozoa in the hindgut are tightly packed, the residual volume available to the spirochetes, which are either surface-attached or free-swimming, is the small gap between the protozoan surfaces. Because protozoa in *C. secundus* are considerably smaller than in *R. santonensis* and *Z. nevadensis*, the surface-to-volume ratio is much larger, which means that the gut may harbor less hydrogen producers and more hydrogen consumers per unit volume.

The hydrogen emission of embedded guts of *R. santonensis* and *Z. nevadensis* was approximately 30- to 50-fold higher than that of living termites, which indicates that the *in situ* conditions in agarose-embedded guts do not completely resemble the conditions *in vivo*. This is also reflected in the metabolite pools, which were smaller in embedded guts than *in vivo*. One explanation for the increased hydrogen emission would be a decreased hydrogen consumption in the periphery of embedded guts. This could be simply caused by damaging of the wall-associated microbiota owing to the embedding procedure. In addition, hydrogen-oxidizing processes in the gut periphery may be oxygen-limited due to the agarose layer, which should represent a larger diffusion barrier than the thin, highly tracheated epithelial tissue. Higher rates of hydrogen oxidation *in vivo* than in embedded guts would result in lower H_2 concentrations at the gut wall and, as a consequence, also at the gut center. This issue is further complicated by the spiracular control of tracheal gas exchange, which is present in many insects and has been recently documented also for termites (Lighton and Ottesen, 2005 and references therein). Cyclic partial closing and opening of the spiracles would not only affect hydrogen-oxidizing processes by controlling O_2 influx into the gut, but also alter the

diffusion barrier for H_2 efflux, leading to fluctuating hydrogen concentrations in the hindgut.

Conclusions

Fluxes of free H_2 in termite hindguts are enormous. Based on the results of this study, the hydrogen production by the intestinal microbiota was estimated to be in the range of 7–16 μmol H_2 (g termite fresh weight)$^{-1}$ h^{-1}. On a volume basis, this means that 1 m^3 of termite hindgut content produces 9–33 m^3 of H_2 per day (atmospheric pressure). In comparison, the same volume of rumen content produces approximately 10 m^3 of H_2 per day (Hungate, 1967; Wolin *et al.*, 1997). In the rumen, H_2 is mainly used for the production of CH_4, which cannot be used by the cow and is subsequently lost by emission (Miller, 1995). In the termite hindgut, however, most of the H_2 is used for reductive acetogenesis, which adds substantially to the amount of produced acetate, the main energy substrate of the termite. About 80% of the energy stored in the digested wood polysaccharides is recovered as acetate. This makes the termite hindgut not only the smallest but also the most efficient natural bioreactor currently known.

Acknowledgements

This study was supported by a grant from the German Research Foundation and by the Max Planck Society. We are grateful to Jared R Leadbetter and Judith Korb for providing termites, and to Jared R Leadbetter for helpful comments.

References

Austin JW, Szalanski AL, Scheffrahn RH, Messenger MT, Dronnet S, Bagnères A-G. (2005). Genetic evidence for the synonymy of two *Reticulitermes* species: *Reticulitermes flavipes* and *Reticulitermes santonensis*. *Ann Entomol Soc Am* **98**: 395–401.

Bignell DE, Eggleton P. (2000). Termites in ecosystems. In: Abe T, Bignell DE, Higashi M (eds). *Termites: Evolution, Sociality, Symbioses, Ecology*. Kluwer Academic Publisher: Dordrecht, pp 363–387.

Boga H, Brune A. (2003). Hydrogen-dependent oxygen reduction by homoacetogenic bacteria isolated from termite guts. *Appl Environ Microbiol* **69**: 779–786.

Boiangiu CD, Jayamani E, Brugel D, Herrmann G, Kim J, Forzi L *et al.* (2005). Sodium ion pumps and hydrogen production in glutamate fermenting anaerobic bacteria. *J Mol Microbiol Biotechnol* **10**: 105–119.

Brauman A, Kane MD, Labat M, Breznak JA. (1992). Genesis of acetate and methane by gut bacteria of nutritionally diverse termites. *Science* **257**: 1384–1387.

Brauman A, Koenig JF, Dutreix J, Garcia JL. (1990). Characterization of two sulfate-reducing bacteria from the gut of the soil-feeding termite, *Cubitermes speciosus*. *Antonie v Leeuwenhoek* **58**: 271–275.

Breznak JA. (1994). Acetogenesis from carbon dioxide in termite guts. In: Drake HL (ed). *Acetogenesis*. Chapman & Hall: New York, pp 303–330.

Breznak JA. (2000). Ecology of prokaryotic microbes in the guts of wood- and litter-feeding termites. In: Abe T, Bignell DE, Higashi M (eds). *Termites: Evolution, Sociality, Symbiosis, Ecology*. Kluwer Academic Publishers: Dordrecht, pp 209–231.

Breznak JA, Brune A. (1994). Role of microorganisms in the digestion of lignocellulose by termites. *Annu Rev Entomol* **39**: 453–487.

Breznak JA, Switzer JM. (1986). Acetate synthesis from H_2 plus CO_2 by termite gut microbes. *Appl Environ Microbiol* **52**: 623–630.

Brugerolle G, Radek R. (2006). Symbiotic protozoa of termites. In: König H, Varma A (eds). *Soil Biology*. Springer-Verlag: Berlin, pp 243–269.

Brune A. (1998). Termite guts: the world's smallest bioreactors. *Trends Biotechnol* **16**: 16–21.

Brune A. (2006). Symbiotic associations between termites and prokaryotes. In: Dworkin M, Falkow S, Rosenberg E, Schleifer K-H, Stackebrandt E (eds). *The Prokaryotes. An Online Electronic Resource for the Microbiological Community*, 3rd edn. Springer-SBM: New York, http://141.150.157.117:8080/prokPUB/index.htm.

Brune A, Emerson D, Breznak JA. (1995). The termite gut microflora as an oxygen sink: microelectrode determination of oxygen and pH gradients in guts of lower and higher termites. *Appl Environ Microbiol* **61**: 2681–2687.

Brune A, Pester M. (2005). In situ measurements of metabolite fluxes: microinjection of radiotracers into insect guts and other small compartments. In: Leadbetter JR (ed). *Methods in Enzymology*. Elsevier: London, pp 200–212.

Brune A, Stingl U. (2005). Prokaryotic symbionts of termite gut flagellates: phylogenetic and metabolic implications of a tripartite symbiosis. In: Overmann J (ed). *Molecular Basis of Symbiosis*. Springer: Berlin, pp 39–60.

Collins NM, Wood TG. (1984). Termites and atmospheric gas production. *Science* **224**: 84–86.

Cord-Ruwisch R, Seitz HJ, Conrad R. (1988). The capacity of hydrogenotrophic anaerobic bacteria to compete for traces of hydrogen depends on the redox potential of the terminal electron acceptor. *Arch Microbiol* **149**: 350–357.

Drake HL, Küsel K, Matthies C. (2006). Acetogenic Prokaryotes. In: Dworkin M, Falkow S, Rosenberg E, Schleifer K-H, Stackebrandt E (eds). *The Prokaryotes. Ecophysiology and Biochemistry*, 3rd edn, Vol. 2 Springer-SBM: New York, http://141.150.157.117:8080/prokPUB/index.htm.

Dröge S, Limper U, Emtiazi F, Schönig I, Pavlus N, Drzyzga O *et al.* (2005). *In vitro* and *in vivo* sulfate reduction in the gut contents of the termite *Mastotermes darwiniensis* and the rose-chafer *Pachnoda marginata*. *J Gen Appl Microbiol* **51**: 57–64.

Dunn S. (2002). Hydrogen futures: toward a sustainable energy system. *Int J Hydrogen Energy* **27**: 235–264.

Dyall SD, Yan W, Delgadillo-Correa MG, Lunceford A, Loo JA, Clarke CF *et al.* (2004). Non-mitochondrial complex I proteins in a hydrogenosomal oxidoreductase complex. *Nature* **431**: 1103–1107.

Ebert A, Brune A. (1997). Hydrogen concentration profiles at the oxic-anoxic interface: a microsensor study of the hindgut of the wood-feeding lower termite

Reticulitermes flavipes (Kollar). *Appl Environ Microbiol* **63**: 4039–4046.

Fröhlich J, Sass H, Babenzien H-D, Kuhnigk T, Varma A, Saxena S *et al.* (1999). Isolation of *Desulfovibrio intestinalis* sp. nov. from the hindgut of the lower termite Mastotermes darwiniensis. *Can J Microbiol* **45**: 145–152.

Gertz KH, Loeschcke HH. (1954). Bestimmung des Diffusionskoeffizienten von H_2, O_2, N_2, und He in Wasser und Blutserum bei konstant gehaltener Konvektion. *Z Naturforsch Teil B* **9**: 1–9.

Graber JR, Breznak JA. (2004). Physiology and nutrition of *Treponema primitia*, an H_2/CO_2-acetogenic spirochete from termite hindguts. *Appl Environ Microbiol* **70**: 1307–1314.

Graber JR, Leadbetter JR, Breznak JA. (2004). Description of *Treponema azotonutricium* sp. nov. and Treponema primitia sp. nov., the first spirochetes isolated from termite guts. *Appl Environ Microbiol* **70**: 1315–1320.

Hall POJ, Aller RC. (1992). Rapid, small volume, flow injection analysis of ΣCO_2 and NH_4^+ in marine and freshwaters. *Limnol Oceanogr* **37**: 1113–1119.

Hedderich R, Forzi L. (2005). Energy-converting [NiFe] hydrogenases: more than just H_2 activation. *J Mol Microbiol Biotechnol* **10**: 92–104.

Hongoh Y, Ohkuma M, Kudo T. (2003). Molecular analysis of bacterial microbiota in the gut of the termite *Reticulitermes speratus* (Isoptera; Rhinotermitidae). *FEMS Microbiol Ecol* **44**: 231–242.

Hungate RE. (1939). Experiments on the nutrition of *Zootermopsis*. III. The anaerobic carbohydrate dissimilation by the intestinal protozoa. *Ecology* **20**: 230–245.

Hungate RE. (1943). Quantitative analyses of the cellulose fermentation by termite protozoa. *Ann Entomol Soc Am* **36**: 730–739.

Hungate RE. (1967). Hydrogen is an intermediate in the rumen fermentation. *Arch Microbiol* **59**: 158–164.

Inoue T, Murashima K, Azuma J-I, Sugimoto A, Slaytor M. (1997). Cellulose and xylan utilization in the lower termite *Reticulitermes speratus*. *J Insect Physiol* **43**: 235–242.

Kambhampati S, Eggleton P. (2000). Taxonomy and phylogenetics of Isoptera. In: Abe T, Bignell DE, Higashi M (eds). *Termites: Evolution, Sociality, Symbiosis, Ecology*. Kluwer Academic Publishers: Dordrecht, pp 1–23.

Koch AL. (1990). Diffusion: the crucial process in many aspects of the biology of bacteria. In: Marshall KC (ed). *Advances in Microbial Ecology*. Plenum Press: London, pp 37–70.

Kuhnigk T, Branke J, Krekeler D, Cypionka H, König H. (1996). A feasible role of sulfate-reducing bacteria in the termite gut. *System Appl Microbiol* **19**: 139–149.

Leadbetter JR, Breznak JA. (1996). Physiological ecology of *Methanobrevibacter cuticularis* sp. nov. and *Methanobrevibacter curvatus* sp. nov., isolated from the hindgut of the termite *Reticulitermes flavipes*. *Appl Environ Microbiol* **62**: 3620–3631.

Leadbetter JR, Crosby LD, Breznak JA. (1998). *Methanobrevibacter filiformis* sp. nov., a filamentous methanogen from termite hindguts. *Arch Microbiol* **169**: 287–292.

Leadbetter JR, Schmidt TM, Graber JR, Breznak JA. (1999). Acetogenesis from H_2 plus CO_2 by spirochetes from termite guts. *Science* **283**: 686–689.

Lee KE, Wood TG. (1971). *Termites and Soils*. Academic Press: New York, USA.

Lee MJ, Schreurs PJ, Messer AC, Zinder SH. (1987). Association of methanogenic bacteria with flagellated protozoa from a termite hindgut. *Curr Microbiol* **15**: 337–341.

Lighton JRB, Ottesen EA. (2005). To DGC or not to DGC: oxygen guarding in the termite *Zootermopsis nevadensis* (Isoptera: Termopsidae). *J Exp Biol* **208**: 4671–4678.

Messer AC, Lee MJ. (1989). Effect of chemical treatments on methane emission by the hindgut microbiota in the termite *Zootermopsis angusticollis*. *Microb Ecol* **18**: 275–284.

Miller TL. (1995). Ecology of methane production and hydrogen sinks in the rumen. In: Engelhardt WV, Leonhardt-Marek S, Breves G, Gieseke D (eds). *Ruminant Physiology: Digestion, Metabolism, Growth and Reproduction*. Ferdinand Enke Verlag: Stuttgart, pp 317–331.

Nunes L, Bignell DE, Lo N, Eggleton P. (1997). On the respiratory quotient (RQ) of termites (Insecta: Isoptera). *J Insect Physiol* **43**: 749–758.

Odelson DA, Breznak JA. (1983). Volatile fatty acid production by the hindgut microbiota of xylophagous termites. *Appl Environ Microbiol* **45**: 1602–1613.

Odelson DA, Breznak JA. (1985). Nutrition and growth characteristics of *Trichomitopsis termopsidis*, a cellulolytic protozoan from termites. *Appl Environ Microbiol* **49**: 614–621.

Ohkuma M, Noda S, Kudo T. (1999). Phylogenetic relationships of symbiotic methanogens in diverse termites. *FEMS Microbiol Lett* **171**: 147–153.

Ottesen EA, Hong JW, Quake SR, Leadbetter JR. (2006). Microfluidic digital PCR enables multigene analysis of individual environmental bacteria. *Science* **314**: 1464–1467.

Pester M, Brune A. (2006). Expression profiles of *fhs* (FTHFS) genes support the hypothesis that spirochaetes dominate reductive acetogenesis in the hindgut of lower termites. *Environ Microbiol* **8**: 1261–1270.

Pester M, Tholen A, Friedrich MW, Brune A. (2007). Methane oxidation in termite hindguts: absence of evidence and evidence of absence. *Appl Environ Microbiol* **73**: 2024–2028.

Revsbech NP. (1989). Diffusion characteristics of microbial communities determined by use of oxygen microsensors. *J Microbiol Meth* **9**: 111–122.

Revsbech NP, Jørgensen BB. (1986). Microelectrodes: their use in microbial ecology. *Adv Microb Ecol* **9**: 293–352.

Salmassi TM, Leadbetter JR. (2003). Molecular aspects of CO_2-reductive acetogenesis in cultivated spirochetes and the gut community of the termite *Zootermopsis angusticollis*. *Microbiology* **149**: 2529–2537.

Sanderson MG. (1996). Biomass of termites and their emissions of methane and carbon dioxide: a global database. *Global Biogeochem Cycles* **10**: 543–557.

Schink B. (1997). Energetics of syntrophic cooperation in methanogenic degradation. *Microbiol Mol Biol Rev* **61**: 262–280.

Schmitt-Wagner D, Brune A. (1999). Hydrogen profiles and localization of methanogenic activities in the highly compartmentalized hindgut of soil-feeding higher termites (*Cubitermes* spp.). *Appl Environ Microbiol* **65**: 4490–4496.

Seedorf H, Dreisbach A, Hedderich R, Shima S, Thauer RK. (2004). $F_{420}H_2$ oxidase (FprA) from *Methanobrevibacter*

arboriphilus, a coenzyme F_{420}-dependent enzyme involved in O_2 detoxification. *Arch Microbiol* **182**: 126–137.

Shinzato N, Matsumoto T, Yamaoka I, Oshima T, Yamagishi A. (1999). Phylogenetic diversity of symbiotic methanogens living in the hindgut of the lower termite *Reticulitermes speratus* analyzed by PCR and in situ hybridization. *Appl Environ Microbiol* **65**: 837–840.

Sugimoto A, Inoue T, Tayasu I, Miller L, Takeichi S, Abe T. (1998). Methane and hydrogen production in a termite-symbiont system. *Ecol Res* **13**: 241–257.

Tholen A, Brune A. (2000). Impact of oxygen on metabolic fluxes and in situ rates of reductive acetogenesis in the hindgut of the wood-feeding termite *Reticulitermes flavipes*. *Environ Microbiol* **2**: 436–449.

Tokuda G, Lo N, Watanabe H. (2005). Marked variations in patterns of cellulase activity against crystalline- vs. carboxymethyl-cellulose in the digestive systems of diverse, wood-feeding termites. *Physiol Entomol* **30**: 372–380.

Tokuda G, Lo N, Watanabe H, Arakawa G, Matsumoto T, Noda H. (2004). Major alteration of the expression site of endogenous cellulases in members of an apical termite lineage. *Mol Ecol* **13**: 3219–3228.

Tokura M, Ohkuma M, Kudo T. (2000). Molecular phylogeny of methanogens associated with flagellated protists in the gut and with the gut epithelium of termites. *FEMS Microbiol Ecol* **33**: 233–240.

Trinkerl M, Breunig A, Schauder R, König H. (1990). *Desulfovibrio termitidis* sp. nov., a carbohydrate-degrading sulfate-reducing bacterium from the hindgut of a termite. System. *Appl Microbiol* **13**: 372–377.

Watanabe H, Tokuda G. (2001). Animal cellulases. *Cell Mol Life Sci* **58**: 1167–1178.

Wolin MJ, Miller TL, Stewart CS. (1997). Microbe-microbe interactions. In: Hobson PN, Stewart CS (eds). *The Rumen Microbial Ecosystem*. Blackie Academic and Professional: London, pp 478–481.

Wood TG, Sands WA. (1978). The role of termites in ecosystems. In: Brian MV (ed.) *Production Ecology of Ants and Termites*. Cambridge University Press: Cambridge, pp 245–292.

Yamin MA. (1980). Cellulose metabolism by the termite flagellate *Trichomitopsis termopsidis*. *Appl Environ Microbiol* **39**: 859–863.

Yamin MA. (1981). Cellulose metabolism by the flagellate *Trichonympha* from a termite is independent of endosymbiotic bacteria. *Science* **211**: 58–59.

Yang H, Schmitt-Wagner D, Stingl U, Brune A. (2005). Niche heterogeneity determines bacterial community structure in the termite gut (*Reticulitermes santonensis*). *Environ Microbiol* **7**: 916–932.